*Physicochem. Probl. Miner. Process., 54(1), 2018, 10-18*

www.minproc.pwr.wroc.pl/journal/

Physicochemical Problems of Mineral Processing

ISSN 1643-1049


*Received April 26, 2017; reviewed; accepted May 26, 2017*

# A simplified analysis of the effect of nano-asperities on particle-bubble interactions

**Jaroslaw W. Drelich**

Michigan Technological University, Department of Materials Science and Engineering, 1400 Townsend Dr. Houghton, MI 49931, USA

Corresponding author: jwdrelic@mtu.edu (Jaroslaw W. Drelich)

**Abstract:** The interactions of gas bubbles with particles having rough and heterogeneous surfaces are much more complex than the commonly used DLVO – based models predict. The effects of surface roughness on flotation and particle – bubble interactions have been reported many times in the past, although a clear understanding of their origins has been lacking. To explain differences in interactions for spherical hydrophobic particles, a theoretical analysis of the interaction potential was carried out for a model rough particle interacting with a bubble surface in an electrolyte solution in this study. The attractive hydrophobic interaction potential was added to repulsive retarded van der Waals and repulsive electrical double layer interaction potentials. The rough microscopic particles were modeled as spheres decorated with nano-sized asperities. Parameters that reflect common flotation separation systems were selected for testing this theoretical model and computation of the energy barrier applicable to particle – flat bubble surface interactions. It was found that hydrophobic asperities with a height of only several nanometers can reduce the repulsive interaction energy by an order of magnitude. Theoretical analysis also reveals that surface coverage of microscopic particles by nano-sized asperities is important as well.

***Keywords:*** *colloidal interactions, flotation, energy barrier, DLVO model, roughness effect*

## 1. Introduction

Froth flotation of mineral particles from electrolyte solution – based suspensions is controlled by the thermodynamics, kinetics, and hydrodynamics of this three phase system. In order for a mineral particle to attach to a gas bubble and then form a stable particle – bubble aggregate, which can be reported to the froth, the following criteria must be met:

**Criterion I:** particle surface must be of an affinity stronger to the gas phase than to the aqueous phase (thermodynamic condition I), and the area of attachment must be of sufficient dimension for the particle – bubble attachment to be initiated (thermodynamic condition II),

**Criterion II:** particle must remain within range of attractive interaction forces with the gas bubble surface over a time that is sufficient for the aqueous phase film to be displaced with gas phase on the particle surface (kinetic condition), and

**Criterion III:** particle/bubble aggregate must be stable under prevailing flow of liquid in the flotation cell/column (hydrodynamic condition).

An additional criterion could refer to the formation, structure and stability of froth, which is so essential for successful recovery in froth flotation (Farrokhpay, 2011), but it is rarely mentioned when mechanisms of particle flotation are discussed.

Although criteria I-III rule the flotation process through its rate and recovery, manipulation of solution chemistry has been at the forefront of research activities in the last few decades (Fuerstenau and Somasundaran, 2003). By selecting reagents and their concentrations, along with the control of reaction and equilibration times, modifications of mineral particle surfaces and their interactions with

http://dx.doi.org/10.5277/ppmp1801

gas bubbles have been manipulated. The effect of mineral particle size on flotation (Tao, 2004; Miettinen et al., 2010; Jameson, 2010), and to some extent particle shape (Ahmed, 2010; Guven et al., 2015b; Guven and Celik, 2016; Hassas et al., 2016), has also been investigated in the past. However, both topography and heterogeneity of mineral particle surfaces have received much less research attention. A limited incorporation of advanced surface characterization instrumentation into complex mineral processing systems, along with a broad distribution of surface heterogeneity and roughness characteristics anticipated for a large population of mineral particles involved in flotation processes, are to blame. The importance of studying surface heterogeneity and surface heterogeneity distribution in flotation systems was discussed and validated in previous contributions (Drelich and Yin, 2010; Drelich and Wang, 2011). It was shown that interactions involving heterogeneous surfaces are much more important to understanding probabilities of particle – bubble attachment events than predicted by the classical or extended (that include hydrophobic interactions) DLVO models when only area – averaged surface charge or potential are employed.

The experimental effects of particle surface roughness on flotation rate and/or recovery reported in the past have been reviewed in previous contributions (Guven et al., 2015a; Drelich and Bowen, 2015) and will not be repeated here. In brief, enhanced flotation of rough particles has been reported several times (Anfruns and Kitchener, 1977; Ducker et al., 1989; Feng and Aldrich, 2000; Rezai et al., 2010; Yekeler et al., 2004), and is often attributed to surface asperities that boost up rupturing of the intervening liquid film during particle – bubble attachment events. Additional complications arise from the fact that gas nano-bubbles can decorate nonwetted mineral particles, and their nucleation is accelerated inside the roughness of particles (Yang et al., 2003). In most recent studies, nicely executed bubble attachment experiments demonstrated bouncing of bubbles on the "smooth" surface of the hydrophobic Teflon plate (Krasowska and Malysa, 2007), nearly identical to bouncing on hydrophilic glass porous surfaces (Zawala et al., 2014). On the contrary, gas bubbles attach spontaneously to a rough surface of the hydrophobic polymer (Krasowska and Malysa, 2007). The enhanced bubble attachment to a rough surface was attributed to the presence of nucleated micro-/nano-bubbles in openings between asperities. Strong repulsive electrical double layer forces might also inhibit the bubbles from attachment to solid surfaces, including hydrophobic surfaces (Krasowska and Malysa, 2007).

In two previous contributions (Guven et al., 2015a; Drelich and Bowen, 2015), a new theoretical analysis of the particle – surface interactions was demonstrated for rough particles. This new analysis revealed changes in particle – surface interaction energies that could be used to explain qualitatively many flotation results reported for rough particles. Specifically, the theoretical analysis suggests that nano-asperities of mineral particles reduce particle – bubble energetic barriers associated with repulsive electrical double layer interactions. In this contribution, a new and simplified theoretical model is introduced. The results of analysis using this simplified model further confirm that surface nano-asperities reduce the magnitude of the particle – bubble energy barrier. It also leads to the conclusion that a low particle surface coverage with hydrophobic nano-asperities has a stronger effect on the particle – bubble attachment energy barrier than higher coverage. Finally, the theoretical model predicts that 40-60% coverage of mineral particles with a hydrophobic collector has a nearly identical effect on attractive hydrophobic interactions as full monolayer coverage.

## 2. Theoretical model

The model of a rough spherical particle interacting with a flat (and rigid) surface of a gas bubble is shown in Figure 1. A mineral particle with a diameter $D = 2R$ is covered with asperities having height $\epsilon_S$ and surface area equal to $2\pi(R + \epsilon_S)\epsilon_S$. The density of asperities per unit surface area of the sphere is denoted as $n$. These nano-asperities cover the particle surface with the fractional area coverage denoted as $\theta$. As a result, the correlation between surface coverage ($\theta$) and the number density of asperities per unit surface area of the sphere ($n$) is:

$$\theta = 2n\pi(R + \epsilon_S)\epsilon_S. \tag{1}$$

The total interaction potential for interactions involved between the particle and gas bubble surface include all three components characteristic to flotation systems: retarded van der Waals ($E_{vdW}$), electrical double layer ($E_{EDL}$) and hydrophobic ($E_H$) interaction potentials. Deformation and elasticity

of the gas bubble is ignored in this modeling in order to simplify the analysis of interactions. Further, according to the model adopted in this study, each of the three interaction potentials are divided for contributions from the $D$ sphere and asperities. The asperities are contoured by a sphere $D_{Asp}$ = 2($R$+ $\epsilon_S$) (Fig. 1). Therefore, as per general relation:

$$E_{Total} = (1-\theta)E(D) + \theta E(D_{Asp}), \quad (2)$$

where $E$ is the interaction potential and refers to either retarded van der Waals, electrical double layer or hydrophobic interactions.

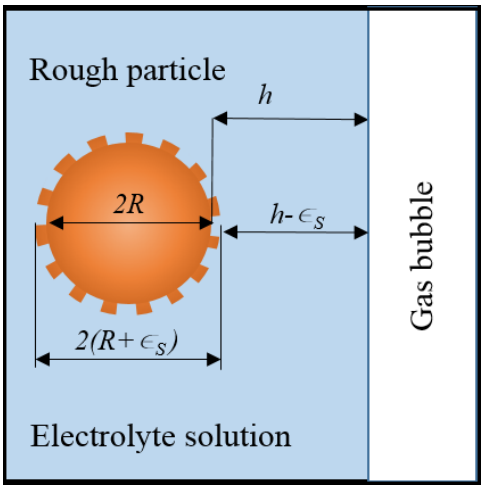


Fig. 1. A schematic of rough particle interacting with non-deformable surface of a gas bubble

The analytical solution of interaction potential for the retarded van der Waals interactions involved between a spherical particle and a flat surface ($S$) was derived by Suresh and Walz using the general pairwise additivity approach and is as follows for a sphere with radius $R$ (Suresh and Walz, 1996):

$$E_{vdW} = 2\pi RA\left[\frac{-2.45\lambda}{120\pi^2h^2} + \frac{2.17\lambda^2}{720\pi^3h^3} - \frac{0.59\lambda^3}{3360\pi^4h^4}\right], \quad (3)$$

where $A$ is the Hamaker constant, [J]; $R$ is the radius of the spherical particle, [m]; $\lambda$ is the characteristic wavelength, [m]; and $h$ is the separation distance as measured from the surface of the spherical particle, [m].

The interaction potential for the electrical double layer interactions used in this study is described by the following equation (Suresh and Walz, 1996):

$$E_{EDL} = 16R(4\pi\epsilon\epsilon_0)\left(\frac{kT}{e}\right)^2 tanh\left(\frac{e\psi_1}{4kT}\right) tanh\left(\frac{e\psi_2}{4kT}\right) e^{-\kappa h} \quad (4)$$

where $\psi 1$ and $\psi 2$ are the surface potentials for a gas bubble surface and a particle, respectively, [V]; $k$ is the Boltzmann constant (1.38×10$^{-23}$ m$^2$ kg s$^{-2}$ K$^{-1}$); $e$ is the electronic charge (1.602×10$^{-19}$ C); $T$ is the temperature (298 K); $\kappa^{-1}$ is the Debye length, [m]; $\varepsilon$ is the bulk dielectric constant (80); and $\varepsilon_0$ is the permittivity of free space (8.85×10$^{-12}$ C$^2$ J$^{-1}$ m$^{-1}$).

The expression for the interaction potential for hydrophobic effects operating between a spherical particle and a smooth surface is (Drelich and Bowen, 2015):

$$E_H = -4\pi R\gamma_{hw}H_yD_H exp\left(\frac{-h}{D_H}\right), \quad (5)$$

where $\gamma_{hw}$ is the hydrophobic surface/water interfacial tension, [J/m$^2$]; $H_y$ (=1) is the Hydra parameter (Donaldson et al., 2015), [unitless]; and $D_H$ is the decay length for hydrophobic interactions, [m].

### 3. Interaction potential and energy barrier for model particles

Energy barriers associated with repulsive electrical double layer interactions (and to a smaller extent with repulsive van der Waals interactions, characteristic to mineral flotation systems), when operating between mineral particles and gas bubbles, either prevent or slow down the rate of flotation (Laskowski et al., 1991). Little attention was given in the past, however, to the analysis and

quantification of energy barriers in mineral processing systems. The theoretical modelling of energy barriers is an important milestone in this direction and is discussed in the following section. Two previous publications, but on spherical particles covered with hemi-spherical asperities (Drelich and Bowen, 2015; Guven et al., 2015a), addressed this issue as well.

### 3.1 Significance of hydrophobic attractive interactions

Figure 2A shows the changes in total, retarded van der Waals, and electrical double layer interaction potentials for varying separations between a spherical particle and a rigid surface. Parameters selected are listed in the figure caption and they are characteristic of mineral flotation systems as discussed earlier (Drelich and Bowen, 2015). A Debye length of $\kappa^{-1}$ = 4.3 nm reflects the 0.005M 1:1 electrolyte solution.

As shown in Fig. 2A, the positive values of the interaction potential for electrical double layer forces indicate their repulsive nature. The van der Waals interactions are repulsive at larger separations but they become attractive at distances between about 0.2 and 2 nm. The energy barrier preventing the mineral particle from attaching to the gas bubble surface is represented by the area above the x-axis and under the line of the total interaction potential. The maximum value for the total interaction potential is about 3250 kT/μm and is located at 1.3 nm distance between the particle and gas bubble surfaces. It is more convenient to discuss the energy barrier in terms of maximum interaction potential value and its location than area under the peak, and this simplified interpretation of the energy barrier is adopted throughout the entire paper.

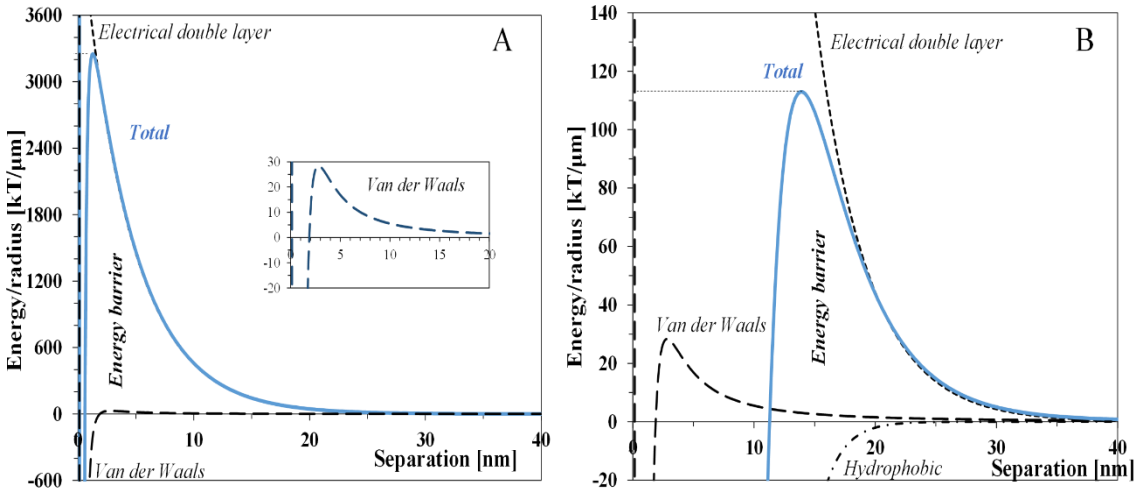


Fig. 2. Interaction potential versus separation curves for A) DLVO interactions and B) DLVO plus hydrophobic interactions between a spherical particle ($D$ = 150 μm) and a flat gas bubble surface. The total interaction potential (solid blue) is the result of retarded van der Waals (dashed), electrical double layer (long dash), and hydrophobic interactions (dash-dot). The following parameters were used: i) for van der Waals interactions ($A$ = -1.3 kT, $\lambda$ = 40 nm); ii) for electrical double layer interactions ($\psi 1$ = - 50 mV, $\psi 2$ = - 50 mV, $\kappa^{-1}$ = 4.3 nm); and iii) for hydrophobic interactions ($D_H$ = 1.7 nm, $\gamma_{mw}$= 50 mJ/m$^2$)

Hydrophobization of the mineral particle surface through adsorption of collectors is a well-recognized principle in flotation of minerals. It involves a number of steps including: *i*) adsorption of individual collectors on selected mineral surface sites, *ii*) formation of hemi-micelles and aggregates, *iii*) completion of formation of a monolayer, and *iv*) formation of structures beyond monolayer (see (Drelich, 2001) and references cited therein). In other words, collector adsorption dictates the evolution of the heterogeneous patterns made of hydrophobic molecular structures on hydrophilic mineral surfaces at different stages of mineral particle hydrophobization.

Hydrophobic interactions that result from this hydrophobization are attractive and necessary for strong attachment of particles to gas bubbles, although their magnitude and range of operation are not

clearly understood. In this modelling, a simple exponential function was chosen with decay length of $D_H$ = 1.7 nm as per a recent report (Donaldson et al., 2015). For simplicity of modeling, the collector molecules are considered to adsorb with the hydrophobic tail penetrating aqueous phase and rising 1 nm above the mineral surface. The interaction potential for a 150 μm particle with a flat bubble surface as a function of collector coverage is shown in Figure 3.

As shown in Fig. 3, the interaction potential of hydrophobic interactions, resulting from a monolayer coverage (100%), reduces the maximum value for the total interaction potential to ~113 kT/μm and this maximum is located at 14 nm separation between surfaces – as per the specific case considered. This is nearly a 30 times drop in the maximum total interaction potential value. A full coverage of the particle surface by the hydrophobic collector monolayer is not necessary to reduce the energy barrier as shown in Fig. 3. A 40 to 50% surface coverage by 1 nm tall molecular structures of the collector (including hemi-micelles) accomplishes nearly the same drop in maximum value of repulsive interaction potential as the full monolayer coverage.

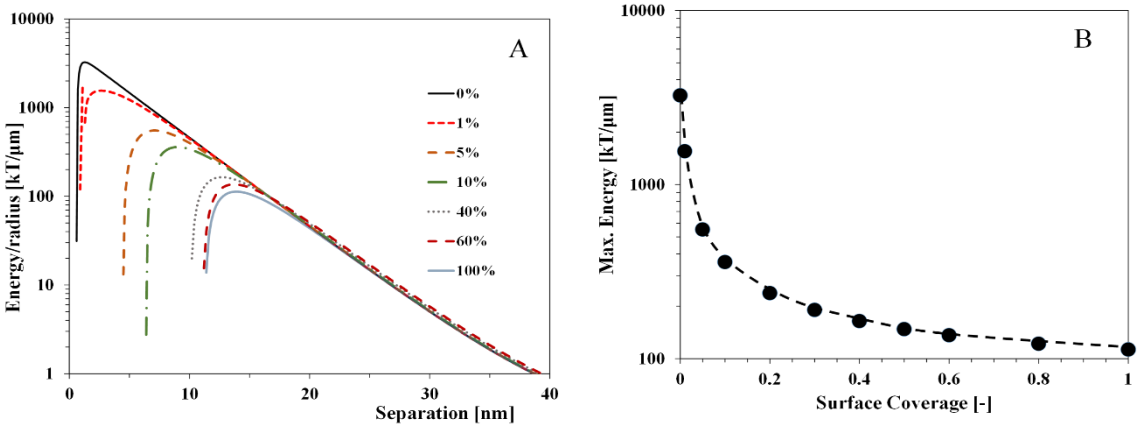


Fig. 3. Interaction potential versus separation curves for a spherical particle ($D$ = 150 μm) covered with hydrophobic hemi-micelles to a different coverage and interacting with a flat gas bubble surface. Hemi-micelles are 1 nm tall. The following parameters were used for both mineral surface and surface of hemi-micelles: i) for van der Waals interactions ($A$ = -1.3 kT, $\lambda$ = 40 nm); and ii) for electrical double layer interactions ($\psi_1$ = -50 mV, $\psi_2$ = -50 mV, $\kappa^{-1}$ = 4.3 nm). For hydrophobic interactions of hemi-micelles the parameters were $D_H$ = 1.7 nm and $\gamma_{mw}$ = 50 mJ/m$^2$. A) Interaction potential (normalized per particle radius) versus separation curves for different coverages of mineral particle by hemi-micelles. B) The effect of particle surface coverage by 1 nm (height) hemi-micelles on the maximum value of the total interaction potential for 150 μm hydrophobic particle interacting with a (rigid) gas bubble surface, normalized per particle radius

### 3.2 Effect of nano-roughness on energy barrier

Figure 4 shows the effect of nano-asperities, having a height of 5 to 20 nm and covering either 1% or 10% of the particle surface, on total interaction potential curves – as normalized per particle radius.

Engineering nano-asperities on the surface of hydrophobic mineral particles changes their interactions with gas bubbles as shown in Fig. 4. Nano-asperities, as small as 5-20 nm, assuming that they are capable of penetrating a particle – gas bubble aqueous film due to either inertial and/or thermal effects, influence interactions drastically. As shown in Fig. 4A, the repulsive electrical double layer and van der Waals forces dominate interactions between mineral particle and gas bubble at larger distances, whereas attractive hydrophobic forces overpower these repulsions at shorter distances. The maximum value for total repulsive interaction potential drops from ~113 kT/μm for the smooth mineral particle to 105, 49, and 4 kT/μm when 1% of the particle surface is covered with 5, 10, and 20 nm asperities, respectively (Fig. 4A). When 10% of the particle surface is covered with 5, 10 or 20 nm asperities, the maximum value of total repulsive interaction potential decreases to 81, 32, or 13 kT/μm, respectively (Fig. 4B).

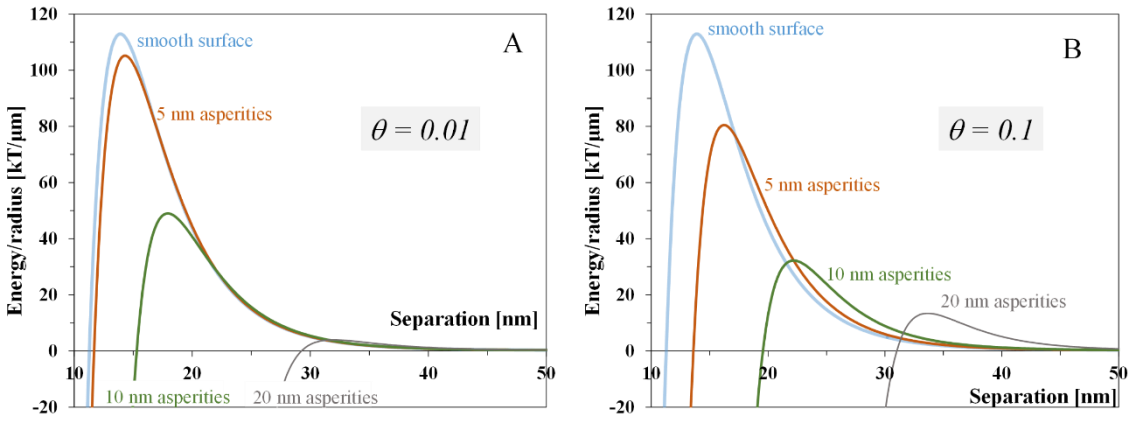


Fig. 4. Total interaction potential for 150 μm hydrophobic particle, with a smooth surface or decorated with 1-20 nm asperities, interacting with a (rigid) gas bubble surface, normalized per particle radius. The coverage with nano-asperioties is $\theta = 0.1$ (A) and $\theta = 0.5$ (B). The parameters used were the same as for Fig. 2

Figure 5 shows the changes in the maximum value of interaction potential for the 150 μm particle that is decorated with 5 nm (height) asperities at a coverage varying from 0 to 100%. The correlation in Figure 5 goes through a minimum at small coverage values and reveals the lowest energy barrier values for small coverage, 5 to 10%. Increasing surface density of 5 nm asperities results in restoration of high values for the energy barrier and is not beneficial for flotation of rough particles.

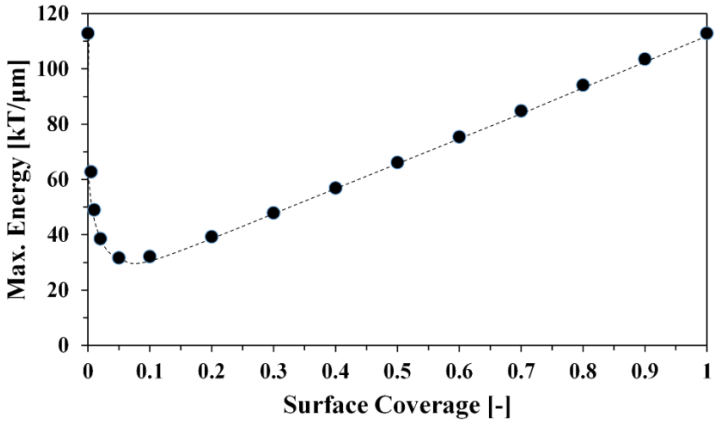


Fig. 5. The effect of particle surface coverage by 5 nm (height) asperities on the maximum value of the total interaction potential for 150 μm hydrophobic particle interacting with a (rigid) gas bubble surface, normalized per particle radius. The parameters used were the same as for Fig. 2

The results in Figs. 4 and 5 clearly indicate that: i) hydrophobic nano-asperities have a very strong effect on the hydrophobic particle – bubble energy barrier of interactions, and an asperity height of only several nanometers can reduce this energy barrier by more than an order of magnitude; and ii) particle surface coverage by nano-asperities also influences the interactions, although this effect is asperity size dependent and non-linear. In general, low coverage by nano-asperities appears to reduce rough particle – gas bubble interactions more than higher surface density of nano-asperities.

### 3.3 Limitation of theoretical analysis

The effect of nano-asperities on particle-bubble interactions, and resulting reduction in energy barrier, can benefit systems in which a thin water film separating mineral surface from gas bubble surface can be reduced to dimensions of colloidal interactions. In many practical systems, structural capillarity effects associated with instability of aqueous films on mineral particles will dominate colloidal

stability, forcing these films to break before their thickness reaches a few tenths of a nanometer. The stability of such films is governed by the competition between interfacial tensions of the solid/liquid/gas system (Sharma and Ruckenstein, 1989). The liquid films rupture suddenly on nonwetting solid surfaces at a critical thickness through formation of a primary hole and its expansion. The liquid film destabilization on mineral surfaces is activated by external vibrations, impurities of liquid film, adsorption of multivalent cations or surfactants at the solid surface, solid surface defects, gradients in liquid film composition concentration, etc.

Theoretical and experimental studies done on stability of aqueous films over macroscopic surfaces shed some important light on the benefits for flotation systems. For example, Sharma and Ruckenstein analyzed the change in free energy of the three-phase system associated with the rupture of a uniform liquid film separating a solid surface from a gas phase (Sharma and Ruckenstein, 1989). They found that the critical film thickness ($h$) at rupture depends on the diameter of the hole (the hole is referred to as a solid area exposed to a gas phase after film rupture) that is formed ($d$) and wetting characteristics of the solid surface defined by the equilibrium contact angle ($\theta$):

$$\frac{4h}{d\sin\theta} = 1 + \frac{(1-\cos\theta)^2}{\sin^2\theta} exp\left(\frac{4h}{d\sin\theta}\right). \quad (6)$$

This formula was later approximated and simplified to (Sharma and Ruckenstein, 1990):

$$d = \frac{2h}{(1-\cos\theta)}. \quad (7)$$

Figure 6 shows a correlation between $d$ and $h$ based on Equation (7) for three mineral surfaces of different wetting characteristics, with a water contact angle of 30, 50 and 70 degrees. These theoretical curves suggest that for a typical range of hydrophobic interactions (10-20 nm), the mineral particle area needed for formation of contact with a gas bubble ($d$ value) is of sub-microscopic dimension, 60-300 nm. Such geometrical conditions are only satisfied for either very fine mineral particles or particles so irregular that only small surface segments with dimensions of 60-300 nm participate in attachment with bubbles. Because mineral particles that are typically separated in froth flotation have a diameter from a few tenths to a few hundredths of a micrometer, the linear dimension of mineral-gas contact area after attachment is usually 1-2 orders of magnitude bigger than the calculated $d$ value. In other words, water films with thickness much exceeding the calculated range of colloidal forces can rupture on surfaces of typical hydrophobized mineral particles, unless their shapes and surfaces are very irregular.

Further, the theoretical models proposed by Sharma and Ruckenstein are limited to water films on smooth solid surfaces. Likely, stability of thin water films changes on rough solid surfaces, including surfaces with nano-sized roughness characteristics – in agreement with experiments for gas bubbles bouncing on smooth and rough surfaces of the hydrophobic polymer (Krasowska and Malysa, 2007). Nano-roughness can have even a more pronounced structural effect on the stability of thin water films than on colloidal interactions and deserves detailed theoretical and experimental studies in the future.

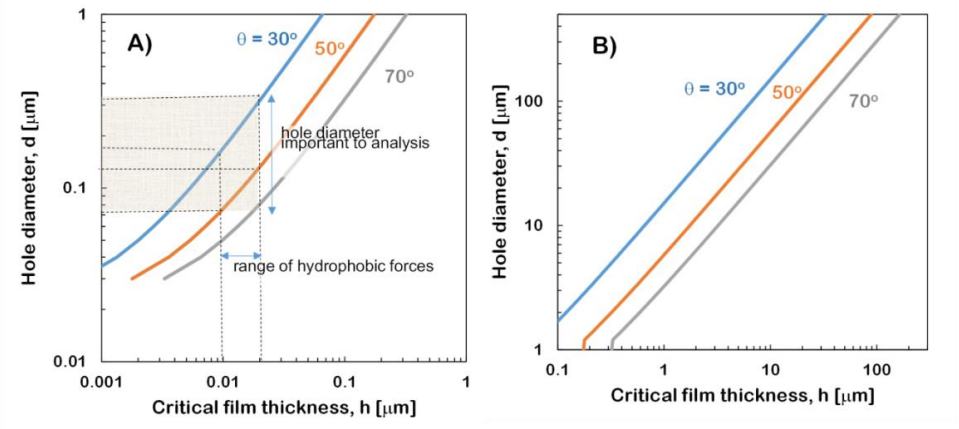


Fig. 6. The diameter of bubble-particle contact area as a function of a critical film thickness that breaks during attachment. The two graphs correspond to two different ranges of film thickness: A) 1 nm to 1 μm, and B) 0.1 to 100 μm

## 4. Conclusion

A simple model of a spherical particle decorated with nano-sized asperities was presented in this contribution. The expressions describing repulsive forces—retarded van der Waals and electrical double layer forces (DLVO interactions)–were adopted from previous work (Suresh and Walz, 1996). The DLVO model was expanded in this study to include attractive hydrophobic interactions, and changes in the interaction potential between a 150 μm particle and the flat and rigid surface of a gas bubble were analysed as a function of the height and surface coverage of asperities. A theoretical analysis revealed that the magnitude of the particle – surface energy barrier decreases with increasing asperity size. The particle – surface energy barrier, caused by repulsive electrical double layer interactions, decreases by more than an order of magnitude when only 1% of the particle is covered with asperities having a 20 nm height. The surface coverage of particles by asperities also has an effect on the energy barrier value and should be considered in addition to the asperity size.

**References**

AHMED, M. M., 2010. *Effect of comminution on particle shape and surface roughness and their relation to flotation process*. International Journal of Mineral Processing, 94 (3-4), 180-191.

ANFRUNS, J. F., KITCHENER., J. A., 1977. *Rate of capture of small particles in flotation*. IMM Trans. Sect. C Miner. Process. Extra. Metall., 86, 9-15.

DONALDSON, S. H., ROYNE, JR., A., KRISTIANSEN, K., RAPP, M. V. , DAS, S., GEBBIE, M. A., LEE, D. W., STOCK, P., VALTINER, M., ISRAELACHVILI, J., 2015. *Developing a general interaction potential for hydrophobic and hydrophilic interactions*. Langmuir, 31, 2051-2064.

DRELICH, J., 2001. *Contact angles measured at mineral surfaces covered with adsorbed collector layers*. Minerals & Metallurgical Processing, 18 (1), 31-37.

DRELICH, J., BOWEN, P. K., 2015. *Hydrophobic nano-asperities in control of energy barrier during particle-surface interactions*. Surface Innovations, 3 (3), 164-171.

DRELICH, J., WANG, Y. U., 2011. *Charge heterogeneity of surfaces: Mapping and effects on surface forces*. Advances in Colloid and Interface Science, 165 (2), 91-101.

DRELICH, J., YIN, X. H., 2010. *Mapping charge-mosaic surfaces in electrolyte solutions using surface charge microscopy*. Applied Surface Science, 256 (17), 5381-5387.

DUCKER, W. A., PASHLEY, R. M., NINHAM, B. W., 1989. *The flotation of quartz using a double-chained cationic surfactant*. Journal of Colloid and Interface Science, 128 (1), 66-75.

FARROKHPAY, S., 2011. *The significance of froth stability in mineral flotation - A review*. Advances in Colloid and Interface Science, 166 (1-2), 1-7.

FENG, D., ALDRICH, C., 2000. *A comparison of the flotation of ore from the Merensky Reef after wet and dry grinding*. International Journal of Mineral Processing, 60 (2), 115-129.

FUERSTENAU, M. C., SOMASUNDARAN, P., 2003. *Flotation*. In Principles of Mineral Processing, edited by M. C. Fuerstenau and K. N. Han. Littleton, CO: Society for Mining, Metallurgy, and Exploration, Inc. (SME), 245-306.

GUVEN, O., CELIK, M. S., 2016. *Interplay of Particle Shape and Surface Roughness to Reach Maximum Flotation Efficiencies Depending on Collector Concentration*. Mineral Processing and Extractive Metallurgy Review, 37 (6), 412-417.

GUVEN, O., CELIK, M. S., DRELICH, J. W., 2015a. *Flotation of methylated roughened glass particles and analysis of particle-bubble energy barrier*. Minerals Engineering, 79, 125-132.

GUVEN, O., OZDEMIR, O., KARAAGACLIOGLU, I. E., CELIK, M. S., 2015b. *Surface morphologies and floatability of sand-blasted quartz particles*. Minerals Engineering, 70, 1-7.

HASSAS, B. V., CALISKAN, H., GUVEN, O., KARAKAS, F., CINAR, M., CELIK, M. S., 2016. *Effect of roughness and shape factor on flotation characteristics of glass beads*. Colloids and Surfaces A: Physicochemical and Engineering Aspects, 492, 88-99.

JAMESON, G. J., 2010. *Advances in Fine and Coarse Particle Flotation*. Canadian Metallurgical Quarterly, 49 (4), 325-330.

KRASOWSKA, M., MALYSA K.. 2007. *Kinetics of bubble collision and attachment to hydrophobic solids: I. Effect of surface roughness*. International Journal of Mineral Processing, 81 (4), 205-216.

LASKOWSKI, J. S., XU, Z., YOON, R. H., 1991. *Energy barrier in particle-to-bubble attachmet and its effect on flotation kinetics*. Paper read at XVIIth International Mineral Processing Congress, at Dresden, Germany, Sept. 23-28, 1991.

MIETTINEN, T., RALSTON, J., FORNASIERO, D., 2010. *The limits of fine particle flotation*. Minerals Engineering, 23 (5), 420-437.

REZAI, B., RAHIMI, M., ASLANI, M. R., ESLAMIAN, A., DEHGHANI, F., 2010. *Relationship between surface roughness of minerals and their flotation kinetics*. In Proceedings of the XI International Mineral Processing and Technology Congress, 232-238.

SHARMA, A., RUCKENSTEIN, E., 1989. *Dewetting of solids by the formation of holes in macroscopic liquid-films*. Journal of Colloid and Interface Science, 133 (2), 358-368.

SHARMA, A., RUCKENSTEIN, E., 1990. *Energetic criteria for the breakup of liquid-films on nonwetting solid surfaces*. Journal of Colloid and Interface Science, 137 (2), 433-445.

SURESH, L., WALZ, J. Y., 1996. *Effect of surface roughness on the interaction energy between a colloidal sphere and a flat plate*. Journal of Colloid and Interface Science, 183 (1), 199-213.

TAO, D. 2004. *Role of bubble size in flotation of coarse and fine particles - A review*. Separation Science and Technology, 39 (4), 741-760.

YANG, J. W., DUAN, J. M., FORNASIERO, D., RALSTON, J., 2003. *Very small bubble formation at the solid-water interface*. Journal of Physical Chemistry B, 107 (25), 6139-6147.

YEKELER, M., ULUSOY, U., HICYILMAZ, C., 2004. *Effect of particle shape and roughness of talc mineral ground by different mills on the wettability and floatability*. Powder Technology, 140 (1-2), 68-78.

ZAWALA, J., KOSIOR, D., MALYSA, K., 2014. *Air-assisted bubble immobilization at hydrophilic porous surface*. Surface Innovations, 2 (4), 235-244.